An Unusual Ferryl Intermediate and its Implications for the Mechanism of Oxacyclization by the Loline-Producing Iron(II)- and 2-Oxoglutarate-Dependent Oxygenase, LolO

Juan Pan,[1,4,6] Eliott S. Wenger,[1,4,7] Chi-Yun Lin,[1] Bo Zhang,[1,8] Debangsu Sil,[1,9] Irene Schaperdoth,[1,10] Setareh Saryazdi,[3,11] Robert B. Grossman,[3] Carsten Krebs,[1,2,5] J. Martin Bollinger, Jr.[1,2,5]

[1]Department of Chemistry and [2]Department of Biochemistry and Molecular Biology, The Pennsylvania State University, University Park, Pennsylvania 16802, United States

[3]Department of Chemistry, The University of Kentucky, Lexington, Kentucky 40506, United States

[4]Equal contributors/co-first authors

[5]Corresponding authors

[6]Present address: New England Biolabs, Ipswich, Massachusetts 01938, United States

[7]Present address: Department of Chemistry, University of Pennsylvania, Philadelphia, Pennsylvania 19104, United States

[8]Present address: The Janssen Pharmaceutical Companies of Johnson & Johnson, Spring House, Pennsylvania 19477, United States

[9]Present address: Department of Chemistry, Indian Institute of Science Education and Research, Pune 411008, India

[10]Present address: Department of Engineering, Dartmouth College, Hanover, New Hampshire 03755, United States

[11]Present address: College of Pharmacy, University of Kentucky, Lexington, Kentucky 40506, United States

Table of Contents Figure

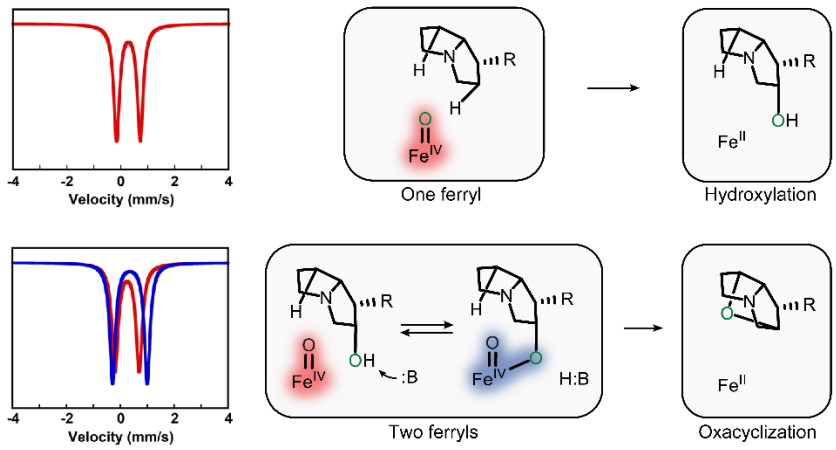

Abstract

N-Acetylnorloline synthase (LolO) is one of several iron(II)- and 2-oxoglutarate-dependent (Fe/2OG) oxygenases that catalyze sequential reactions of different types in biosynthetic pathways that provide valuable natural products. LolO hydroxylates C2 of 1-*exo*-acetamidopyrrolizidine before coupling the C2-bonded oxygen to C7 to form the tricyclic (nor)loline core. Each reaction requires abstraction of hydrogen (H•) from carbon by an oxoiron(IV) (ferryl) intermediate, but different sites are targeted, and the carbon radicals have different fates. There have been prior indications that the disposition of the substrate and the intermediate in the active site controls the site of H• abstraction and can impact the fate of the radical in related enzymes. These indications led us to determine whether active-site reconfiguration in the second LolO-catalyzed reaction might contribute to the observed change in the outcome. Whereas the single ferryl complex in the C2 hydroxylation reaction was previously shown to have typical Mössbauer parameters, the second of two ferryl complexes to accumulate during the oxacyclization step has an isomer shift greater than that of any such complex characterized to date in an Fe/2OG enzyme. Moreover, it abstracts H• from C7 ~20 times faster than does the first ferryl complex in its previously reported off-pathway hydroxylation of C7. The detectable hydroxylation of C7 in competition with cyclization by the *second* ferryl complex is not enhanced in $^{2}H_2O$ solvent, suggesting that the C2 hydroxyl is deprotonated prior to C7–H cleavage. These observations are consistent with coordination of the C2 oxygen to the second ferryl complex, which may reorient its oxo ligand, the substrate, or both to positions more favorable for C7–H cleavage and cyclization.

Introduction

In mammals, iron(II)- and 2-oxoglutarate-dependent (Fe/2OG) dioxygenases (hydroxylases) catalyze reactions essential for connective tissue synthesis, epigenetic regulation, and oxygen and body-mass homeostasis. In plants and microbes, Fe/2OG di- and *mono*oxygenases promote hydroxylation, halogenation, stereoinversion, desaturation, cyclization, ring expansion, fragmentation, epoxidation, and endoperoxidation of their substrates in primary and specialized metabolic pathways.[1-12] Nature has adapted a single protein architecture, known as the cupin or jellyroll fold, for this array of outcomes.[13] At its heart is a mononuclear non-heme Fe(II) cofactor that is coordinated by a pair of cis-disposed histidine ligands.[14] In the majority of cases, a carboxylate from an aspartate or glutamate residue completes a "facial triad" of protein ligands that leaves the three sites on the opposite octahedral face available for coordination of the class-defining cosubstrates, 2OG and O_2.[14] 2OG chelates via its C2 carbonyl oxygen and C1 carboxylate.[15] In a few cases, the absence of the protein carboxylate ligand leaves one additional site unoccupied for coordination of substrates, and, in the most well-studied case of the Fe/2OG aliphatic halogenases, this site coordinates a halide (or another anion in several reported nonnative reactions[16-18]) to enable coupling of this exogenous ligand to a carbon atom of the enzyme-specific "prime substrate."[3,19] Generally, the prime substrate of an Fe/2OG oxygenase does not coordinate directly to the cofactor.[20] It is instead bound nearby, with typical separations between its target site and the iron cofactor of ~ 4-5 Å, by specific non-covalent contacts within the tailored active site.[13] Binding of the prime substrate, which is generally the last step in assembly of the O_2-reactive enzyme•substrates complex, results in dissociation of a water ligand, thereby creating an open coordination site for O_2 addition; this phenomenon has been termed “substrate triggering.”[15,18,21-24]

All Fe/2OG oxygenases that have been studied in depth begin with addition of O_2 to the open site of the Fe(II) cofactor in the enzyme complex with all other substrates bound (**Scheme 1**).[23,25-26] In most of the complete reactant complexes that have been crystallographically characterized, this open site is trans to the C-terminal histidine ligand (His_C).[5,25,27] This site is considered to be "in-line," because it projects toward the target site of the prime substrate. Some structures have shown the carboxylate of 2OG shifted toward or fully into this in-line position, rendering the site trans to the N-terminal histidine ligand (His_N), the “off-line” site, apparently more open for O_2 addition.[24,28-29] In either case, capture of O_2 is presumed to yield a superoxoiron(III) cofactor that has not yet been directly characterized in any Fe/2OG oxygenase but has been trapped in other mononuclear non-heme iron enzymes and model complexes.[30-32] Decarboxylation of 2OG and coupling of its C2 to the distal oxygen of the O_2 ligand then yields a Fe(II)–peroxysuccinate complex that has been crystallographically characterized in the L-arginine 3-hydroxylase, VioC.[25] Heterolysis of the peroxide bond of this complex produces the marquee intermediate of the class, the oxoiron(IV) (ferryl) complex (**Scheme 1**), which has been characterized by Mössbauer spectroscopy in more than 10 different enzymes.[4-5,7,23-24,30,33-36] These intermediates have a high-spin ($S = 2$) electron spin ground state that results in isomer shifts (δ) of 0.22–0.32 mm/s and quadrupole splitting parameters (ΔE_Q) of about –1.0 mm/s, respectively.[7,36-37]

Most commonly, hydrogen atom (H•) transfer (HAT) from the target site of the prime substrate to the ferryl complex generates an intermediate that harbors a carbon-centered radical and hydroxoiron(III) cofactor. The varied pathways through which this common intermediate reacts give rise to the array of chemically distinct outcomes cited above. Attack by the prime-

substrate carbon radical upon the iron-coordinated oxygen that generated it — a step termed "oxygen rebound"[38] — leads to C–O coupling and hydroxylation (**Scheme 1**, *green arrows*).[26] Attack of the substrate radical on a ligand (e.g., halogen, depicted as X in **Scheme 1**) cis to the hydroxyl results in formation of a different carbon–heteroatom bond (*purple arrows*).[23] Several other fates, including HAT or (proton-coupled) electron transfer [(PC)ET] from the substrate

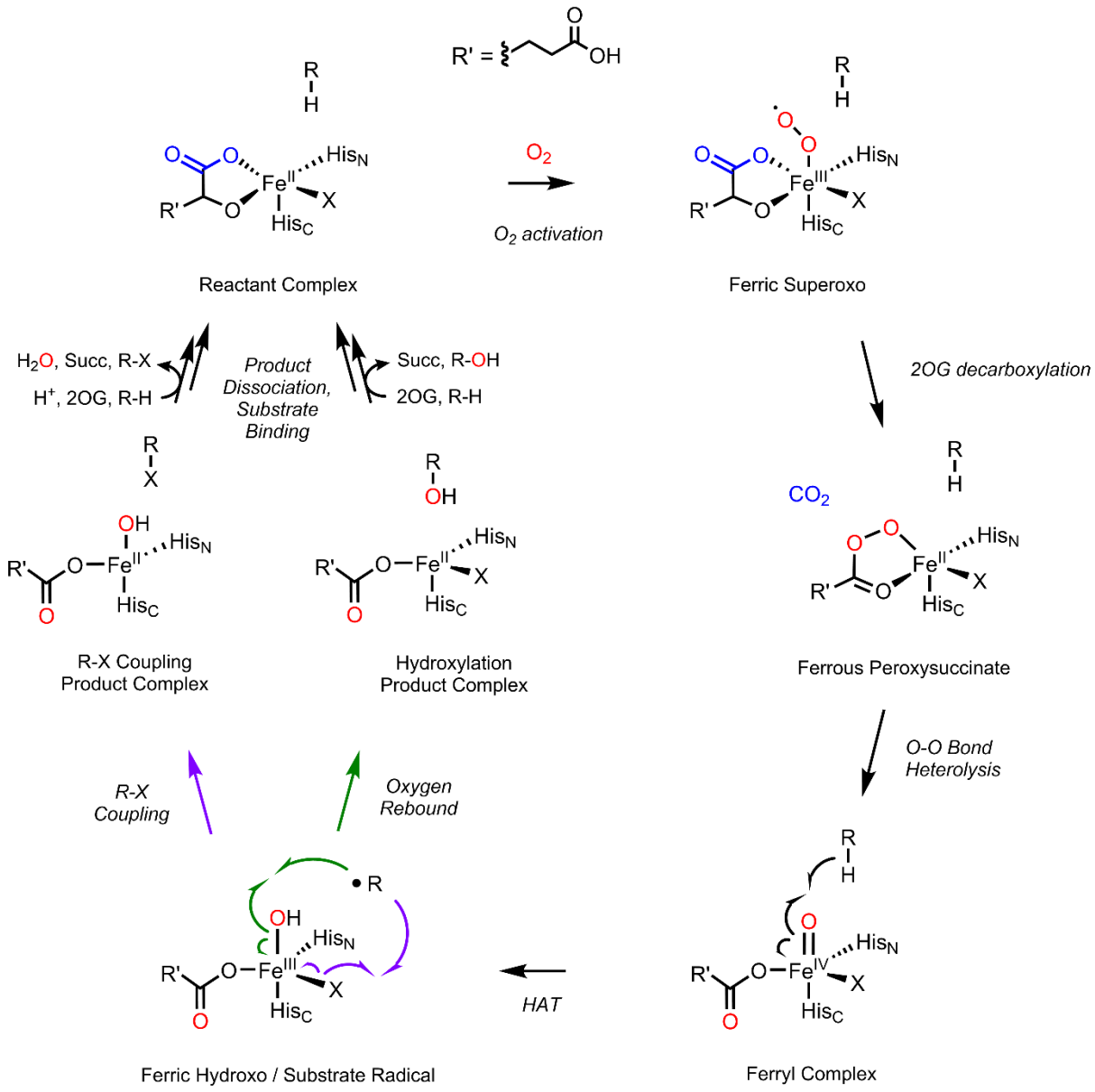

Scheme 1. A generalized Fe/2OG enzyme-catalyzed hydroxylation reaction.

radical to the hydroxoiron(III) cofactor,[5] HAT to the radical from an enzyme tyrosine,[4] capture of O_2 by the substrate radical,[12] and addition of the radical to a neighboring substrate olefin,[39-40] have been shown or proposed to initiate desaturation, decarboxylation, stereoinversion, endoperoxidation, and carbocyclization reactions, respectively.

Early work on the aliphatic halogenase SyrB2 highlighted a unifying chemical challenge that must be surmounted by Fe/2OG enzymes that promote reactions other than hydroxylation: avoidance of the facile oxygen-rebound step.[23] An inverse correlation of the rate of HAT with the ratio of chlorinated to hydroxylated product spurred frontier-orbital analysis that led to the hypothesis that a substrate–ferryl disposition with an Fe–O–H(C) angle approaching 90° results in inefficient HAT but also favors attack of the substrate radical on the cis halogen in preference to

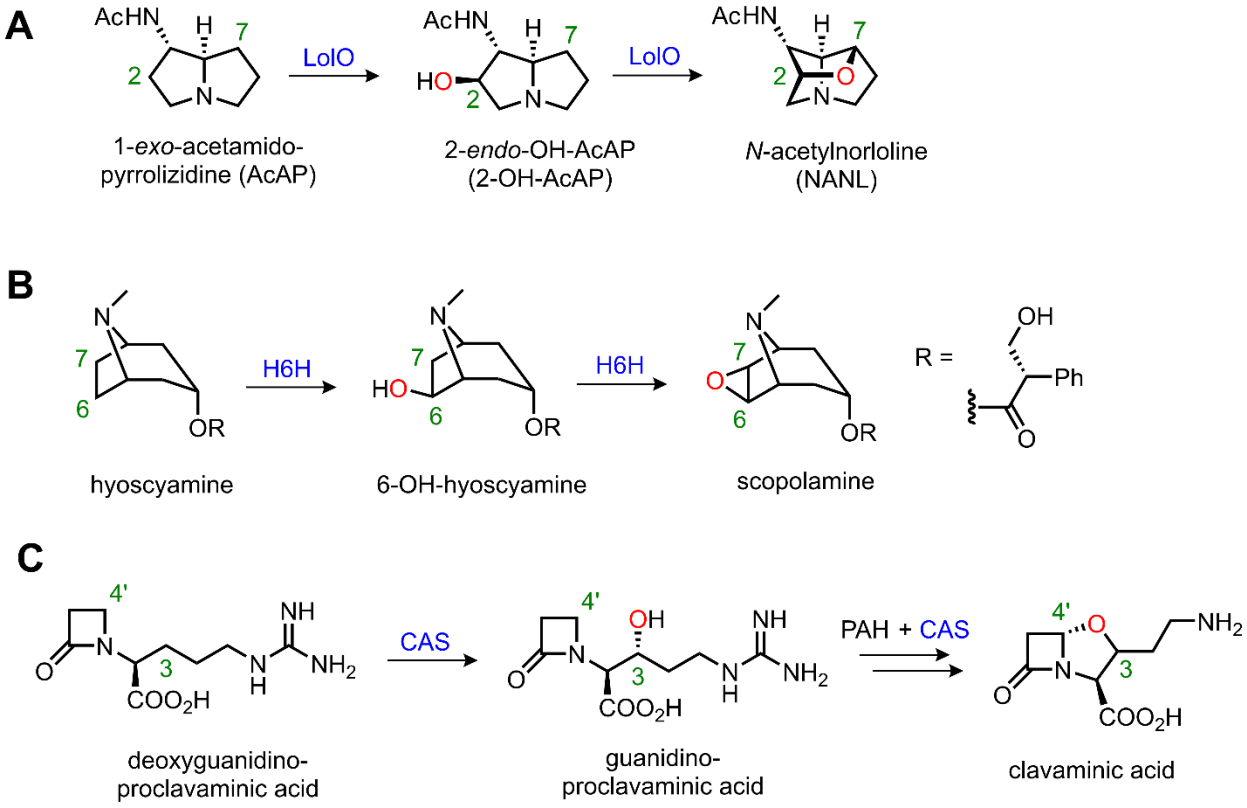

Scheme 2. Hydroxylation and oxacyclization reactions catalyzed by the Fe/2OG oxygenases LolO, H6H, and CAS.

oxygen rebound.[41-43] The prior recognition of the "off-line" 2OG binding mode helped inspire the notion that coordination isomerism of the ferryl complex (i.e., an off-line oxo), rather than relocation of the substrate within the conserved protein architecture, brings about this special disposition of the C–H target of the prime substrate and the H•-accepting ferryl complex.[27,42]

The ability of Fe/2OG enzymes to install useful functional groups upon even completely unactivated aliphatic carbon centers has brought them into the focus of biocatalysis research.[44-45] Development of the versatile scaffold for synthetic processes would be facilitated by an understanding of how specific structural features of a given enzyme select its outcome from among the myriad possibilities. Knowledge of the individual reaction pathways is a prerequisite to such an understanding. In the last two decades, insight has emerged into several of the reaction types, but the mechanisms of conversion of secondary alcohols to oxygen heterocycles (hereafter referred to generally as oxacyclization; **Scheme 2**) are less well understood. Such reactions occur, for example, in the biosyntheses of the fungal insecticides/antifeedants known collectively as lolines

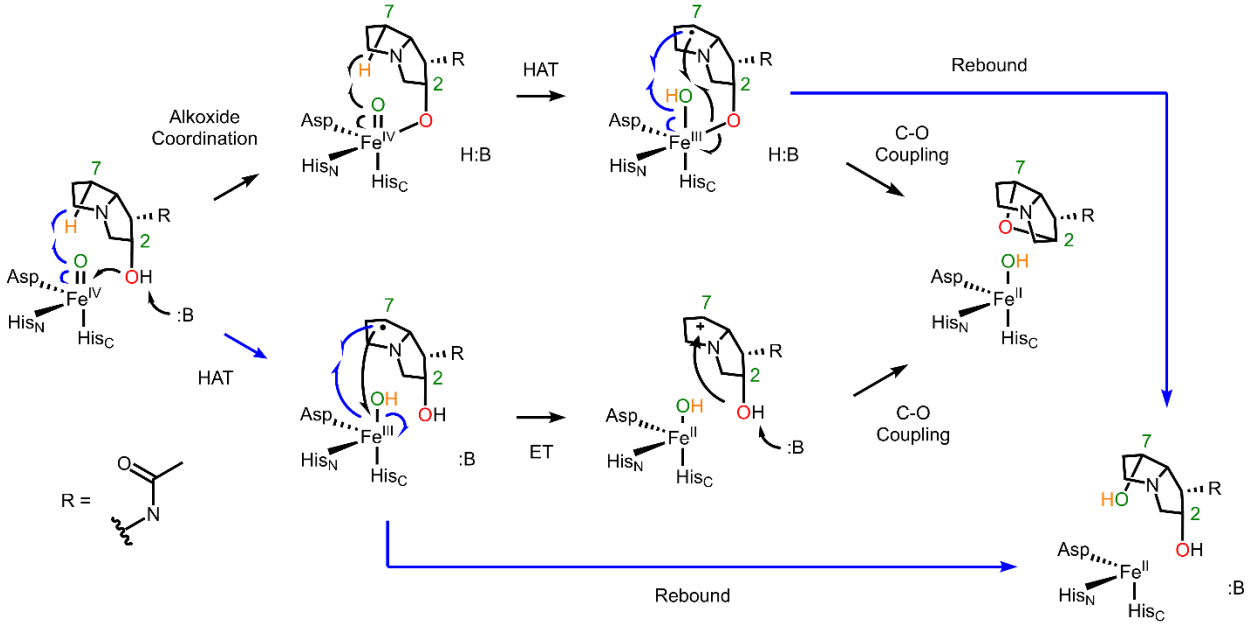

Scheme 3. Possible mechanisms for the oxacyclization reaction catalyzed by LolO.

[by *N*-acetylnorloline (NANL) synthase, LolO; **Scheme 2A**],[7] the plant-derived anesthetic scopolamine (by hyoscyamine 6β-hydroxylase, H6H; **Scheme 2B**),[46-47] and the antibiotic clavulanic acid (by clavaminate synthase, CAS; **Scheme 2C**).[6,29]

One possible pathway would culminate in a radicaloid ring closure, in which the substrate radical generated by the canonical ferryl intermediate would attack a cis-coordinated alkoxide oxygen (**Scheme 3**, *top pathway*), in analogy to the carbon–halogen coupling step in the halogenases and the carbon–sulfur coupling step in the generation of the thiazolidine ring by isopenicillin *N* synthase, a mononuclear non-heme iron enzyme related to the Fe/2OG enzymes.[3,41,48] However, all known oxacyclases retain the complete facial ligand triad; they lack the key adaptation of the halogenases – substitution of the facial triad carboxylate with a non-coordinating residue – that allows for anion coordination to the iron center and enables its subsequent radicaloid coupling to the substrate carbon. Nevertheless, because progression to the ferryl intermediate involves loss (as CO_2) of the C1 carboxylate of 2OG (an iron ligand in the reactant complex), the substrate oxygen could potentially coordinate during or after ferryl formation. Coordination to the Lewis-acidic cofactor could obviate proton transfer from the substrate hydroxyl group in the C–O-coupling step.

In lieu of direct alkoxide coordination, further oxidation of the substrate radical by a (potentially reversible) (PC)ET to the Fe(III)-OH cofactor could form a secondary carbocation, which could undergo polar capture by the substrate oxygen to close the ring (**Scheme 3**, *bottom pathway*). Notably, this mechanism could involve a kinetically significant (i.e., partially rate-determining) alcohol deprotonation step prior to C–O coupling. For LolO, however, previous work has shown that the presence of two fluorines on C6 (which would be expected to preclude carbocation formation at C7) does not block oxacyclization, an observation weighing against a

polar pathway.[49] Regardless of the operant C–O-coupling mechanism, oxygen rebound might be expected to compete with oxacyclization to some extent, as was found to occur, for example, in the halogenases and the desaturase NapI.[5,41] In the event of competitive hydroxylation, quantitative assessment of whether the partition ratio responds to different experimental perturbations might then provide a means to probe the mechanism of the ring-closure step.

The issues of control of the fate of the substrate radical and avoidance of oxygen rebound are especially interesting for the subset of Fe/2OG enzymes that perform multiple reactions – one hydroxylation and one (or more than one) other reaction – in biosynthetic sequences. The three oxacyclases mentioned above (**Scheme 2**) belong to this subset. LolO (**Scheme 2A**), the subject of this study, first hydroxylates C2 of 1-*exo*-acetamidopyrrolizidine and then couples the new C2 oxygen to C7 to install the oxolane moiety of the compact, tricyclic loline core.[7] Analogously, H6H (**Scheme 2B**), which we have investigated in a parallel study,[50] first hydroxylates C6 of hyoscyamine before cyclizing the alcohol to install the C6-C7 epoxide of scopolamine.[46-47] CAS first hydroxylates C3 of deoxyguanidinoproclavaminate before coupling the C3 oxygen to C4′ of the β-lactam ring, although in this case, hydrolysis of the substrate guanidine side chain by a different enzyme interrupts the CAS-catalyzed hydroxylation and oxacyclization reactions (**Scheme 2C**).[6,29]

In each of these three pathways, the site of H• abstraction and the fate of the resulting substrate radical change from the first reaction to the second. Conceivably, the differences in substrate structure for the two steps could change the disposition of the substrate and ferryl complex either by shifting the substrate, altering the coordination geometry of the ferryl intermediate, or both. For example, in an extreme case of such dynamic repositioning, the oxygen of the hydroxylated intermediate could coordinate to the second ferryl complex, shift the

oxacyclization substrate in the active site, and bring the C–H target of the oxacylization step into a position favorable for HAT. At the other extreme, a single, optimized position of the substrate could set the stage for the sequential outcomes. The site of hydroxylation would be positioned more optimally to donate H• to the ferryl complex in the first reaction and appropriately for subsequent rebound. The second site would be positioned (1) so that HAT from it to the ferryl complex would become competitive only after "blocking" of the more facile site by its hydroxylation and (2) at a distance and angle to impede rebound, as seen in the halogenases.[42]

In this study, we probed the mechanism of the oxacyclization reaction catalyzed by LolO and investigated whether the enzyme actively changes the HAT target and outcome from the first (C2 hydroxylation) to the second (C2–O–C7 cyclization) reaction. Unusual Mössbauer-spectroscopic properties of the cyclization-promoting ferryl intermediate, marked enhancement of its rate of C7–H cleavage relative to that of the ferryl complex formed in the first reaction, and insensitivity of the partition ratio between oxacyclization and C7 hydroxylation to deuterated solvent suggest that LolO employs a dynamic repositioning mechanism that most likely involves C2–alkoxide coordination in the second reaction. In the parallel study, contrasting structural and mechanistic observations on the distinct type of oxacyclization catalyzed by H6H (epoxidation versus oxolane formation) lead to the conclusion that it employs a distinct strategy – one exploiting (1) a single optimized substrate–ferryl disposition, (2) the divergent spatial dependencies of HAT and oxygen-rebound steps, and (3) base-assisted ring closure without alkoxide coordination – to direct its sequential hydroxylation and epoxidation reactions.[50] Together, these two studies mirror prior work on olefin-installing desaturations by Fe/2OG oxygenases in reflecting divergent reaction pathways correlated to details of the substrate and product structures of apparently similar reactions.[5]

Results and Discussion

Conversion of 2-OH-AcAP to NANL and a minor dihydroxylated product. Analysis by liquid chromatography coupled to mass spectrometry (LCMS) (**Figure 1**) of a reaction in which (1*S*)-2-*endo*-hydroxy-1-*exo*-acetamidopyrrolizidine (2-OH-AcAP) was incubated with LolO in the presence of Fe(II), 2OG, and O_2 revealed conversion to a new species characterized by a change in mass-to-charge ratio ($\Delta m/z$) of –2 (**Figure 1A**), as expected for the oxacyclization product, NANL. The quantity of NANL generated was found to depend on the concentration of 2OG provided to the enzyme (**Figure 1B**). With a 2OG:2-OH-AcAP ratio of 0.6, approximately half of the substrate was consumed, and the NANL yield exceeded half of its maximum value. With 2OG:2-OH-AcAP = 1.2, the 2-OH-AcAP substrate was almost completely consumed and the NANL product yield was nearly maximized. These observations imply relatively efficient coupling between 2OG decarboxylation and cyclization of the prime substrate (< 20% failure). A small quantity (< 2%) of a species with $\Delta m/z$ +16 was also be detected at the higher extents of conversion enabled by higher 2OG:2-OH-AcAP ratios (**Figure 1A**). The results imply that LolO preferentially cyclizes 2-OH-AcAP but, in competition, also hydroxylates it to a minor extent (at C7; see below), as has been seen previously with other Fe/2OG enzymes (e.g., halogenases and H6H).[41,50-51] When LolO cyclization reactions were conducted under $^{18}O_2$, the $\Delta m/z$ of the primary NANL product was not affected, as expected for the coupling of the extant C2–O to C7 in formation of the cyclic ether (**Figure 1A**). However, the minor product, previously at $\Delta m/z$ +16, was shifted by two mass units to $\Delta m/z$ +18 (inset of **Figure 1A**), implying that it results from an aberrant second hydroxylation by oxygen rebound. The incorporation of ^{18}O is discussed more quantitatively below.

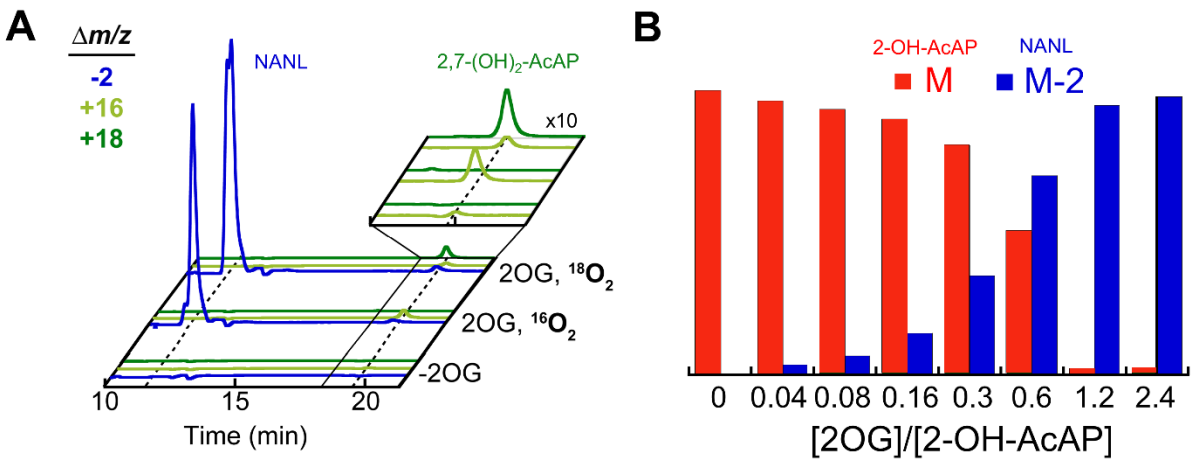

Figure 1. *In vitro* conversion of 2-OH-AcAP to NANL by LolO monitored by liquid chromatography coupled to mass spectrometry (LCMS). (***A***) Chromatograms showing the two products formed by LolO from 2-OH-AcAP: NANL, with Δ*m/z* -2, and 2,7-$(OH)_2$-AcAP, with Δ*m/z* +16. Carrying out the reaction under $^{18}O_2$ resulted in a change in a 2-unit increase in Δ*m/z* for 2,7-$(OH)_2$-AcAP (85% ^{18}O incorporation) but no change in the Δ*m/z* for NANL. (B) Variation of the intensities of LCMS peaks for 2-OH-AcAP (*green*) and NANL (*blue*) in analysis of LolO reactions with varying 2OG:2-OH-AcAP ratio. Reaction conditions are provided in the **Materials and Methods** section of the *Supporting Information*.

Evidence for ferryl-mediated C7–H cleavage in the LolO-catalyzed oxacyclization. To promote its oxacyclization reaction, LolO must cleave both a C7–H bond and the alcohol O–H bond of 2-OH-AcAP. To test the expectation that the C7–H bond is cleaved by the ferryl complex, we compared the kinetics of LolO reactions with 2-OH-AcAP of natural isotopic abundance and 7,7-[$^2H_2$]-2-*endo*-hydroxy-1-*exo*-acetamidopyrrolizidine (7,7-d_2-2-OH-AcAP; **Figure S1**) by stopped-flow absorption (SF-Abs) spectroscopy. As in prior work on Fe/2OG oxygenases, mixing at 5 °C of an

anoxic solution containing the O_2-reactive enzyme•substrates complex [LolO•Fe^{II}•2OG•(7,7-d_2)-2-OH-AcAP] with a buffer solution delivering substoichiometric (limiting) O_2 resulted in both a transient increase in absorbance at 320 nm (A_{320}), reflecting formation and decay of the UV-absorbing ferryl intermediate (**Figure 2**, *light blue circles*), and a transient decrease in A_{510}, reflecting decay and reformation of the LolO•Fe^{II}•2OG•2-OH-AcAP reactant complex (**Figure S2**).[7,26,52] Use of the substrate bearing deuterium on C7 (**Figure 2**, *dark blue circles*) made the amplitude of the ΔA_{320} transient much greater – indicating increased accumulation of the ferryl complex – and slowed its return to the initial value, reflecting a sizeable normal substrate deuterium kinetic isotope effect (D-KIE) on its decay.[7,23,26,52] Qualitatively, these observations imply that the UV-absorbing ferryl complex is responsible for cleaving the C7–H/D bond in the reaction.

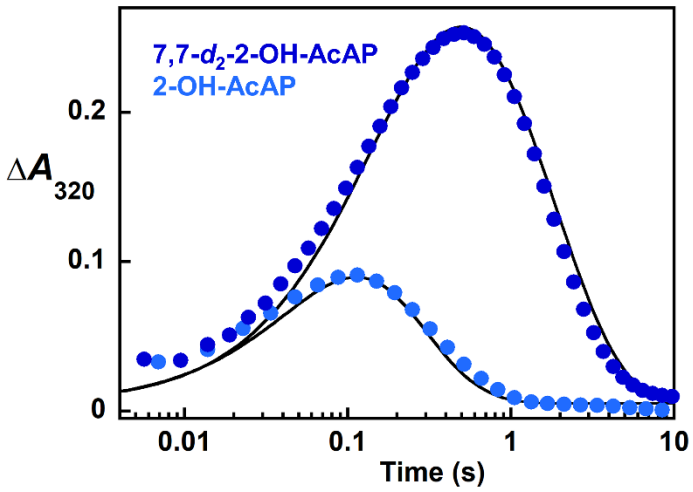

Figure 2. Kinetic evidence of HAT from C7 to the ferryl complex in the oxacyclization reaction catalyzed by LolO. Absorbance at 320 nm was monitored after air-saturated buffer (50 mM sodium HEPES, pH 8, with 5% glycerol) was mixed at 5° C with an equal volume of an O_2-free reactant complex containing LolO (1.75 mM), Fe(II) (1.4 mM), 2OG (7 mM), and 5 mM of either 2-OH-AcAP (*light blue circles*) or 7,7-d_2-2-OH-AcAP (*dark blue circles*). Simulations of the traces according to the model depicted in **Scheme S1** are shown as black lines. These simulations

assumed concentrations of 0.18 mM for O_2 and 0.5 mM for the O_2-reactive LolO•Fe^{II}•2OG•substrate complex (the latter representing an active fraction of 0.7). Fractional reactivity of the enzyme•substrates complex has frequently been encountered in prior studies of Fe/2OG enzymes, including LolO.[7,36,52]

By simulating the ΔA_{320}-*vs*-time traces from reactions with both substrates according to the kinetic model depicted in **Scheme S1**, we estimated a second-order rate constant of 16 $mM^{-1}s^{-1}$ for the bimolecular reaction of O_2 with the reactant complex (through intermediate states that do not accumulate) to form the UV-absorbing ferryl complex and decay rate constants of 19 s^{-1} and 0.8 s^{-1} for the reactions with the protium- and deuterium-bearing substrates, respectively (**Figure 2**, *solid lines*). The large ratio of ~24, which represents a lower limit for the intrinsic D-KIE, confirms that the intermediate abstracts hydrogen from C7. This conclusion is further validated by the $\Delta m/z$ value of the minor 2,7-$(OH)_2$-AcAP product in the reaction with the deuterium-bearing substrate: the +15 change from the m/z of the 7,7-d_2-2-OH-AcAP substrate corresponds to loss of one deuterium atom ($\Delta m/z$ –2), necessarily from C7, in incorporation of the hydroxyl group ($\Delta m/z$ +17) (**Figure S3**).

A previous study of the LolO hydroxylation reaction showed that the enzyme "misfires" in a small fraction of events and hydroxylates C7 instead of C2.[52] A rate constant of 0.7 s^{-1} at 5 °C was deduced for HAT from C7 to the ferryl complex in the off-pathway hydroxylation reaction. In considering the possibility of substrate repositioning for the second reaction, we judged it informative to compare this rate constant to that for cleavage of the C7–H bond of 2-OH-AcAP reflected by the data in **Figures 1** and **2**. The rate constant determined in **Figure 2** (19 s^{-1}) is for decay of the ferryl complex, which represents the sum of all competing pathways – those that result in C7–H cleavage and those that do not. However, the data in **Figure 1** implying < 20%

unproductive decay set a lower limit of 15 s^{-1} for HAT from C7 to the ferryl complex in the oxacyclization reaction. In other words, the presence of the hydroxyl group at C2 accelerates cleavage of the C7–H bond by a factor of at least ~20 (15 s^{-1}/0.7 s^{-1}). In light of the expectation that addition of a C2 hydroxyl group should have no significant effect on the homolytic bond dissociation energy (BDE) of the C7–H bond, and given prior evidence for the primary importance of substrate–intermediate disposition in the efficiency of HAT to the ferryl complex,[41-42] we posit that the observed acceleration reflects a change in the relative disposition of the C7–H and Fe^{IV}=O bonds by either movement of the substrate, a change in the configuration of the ferryl complex, or both.

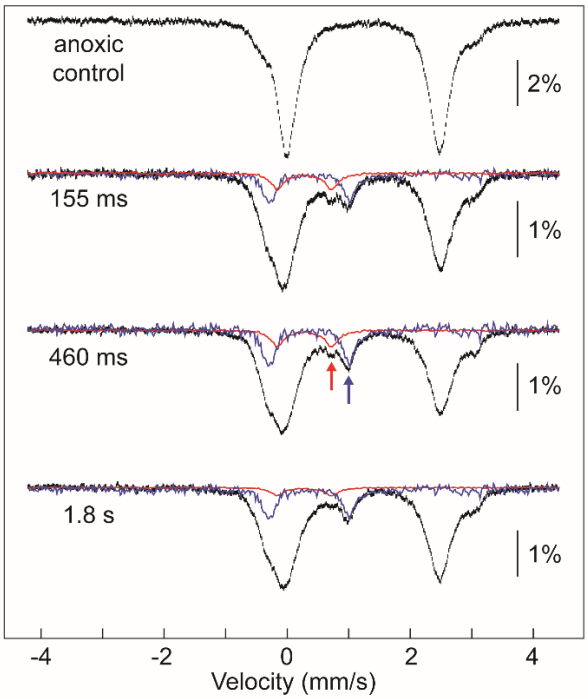

Figure 3. Mössbauer spectra (4.2 K/0 mT) from a freeze-quench (FQ) experiment probing the ferryl complex(es) in the oxacyclization reaction of LolO. The top spectrum is of a frozen solution containing LolO (1.95 mM), $^{57}Fe^{II}$ (1.57 mM), 2OG (7.5 mM), and 7,7-d_2-2-OH-AcAP (7 mM). The bottom three spectra are of samples freeze-quenched at the indicated reaction times after mixing this solution with 0.5 equivalent volume (2:1 mix) of a solution of O_2-

saturated buffer at 5 °C, giving final concentrations of ~ 0.6 mM O_2 and 1 mM ^{57}Fe after mixing. The red and blue lines are experimental reference spectra of the hydroxylation (Fe^{IV}_H) and oxacyclization (Fe^{IV}_O) ferryl intermediates.

Evidence by Mössbauer spectroscopy for two distinct ferryl intermediates in the oxacyclization reaction. To probe the ferryl complex of the oxacyclization reaction directly, we trapped it by the freeze-quench (FQ) method for characterization by Mössbauer spectroscopy (**Figures 3 and S5**). The spectrum of the frozen LolO•Fe^{II}•2OG•7,7-d_2-2-OH-AcAP reactant complex (acquired at 4.2 K with no externally applied magnetic field) exhibits a quadrupole doublet with isomer shift (δ) and quadrupole splitting (ΔE_Q) parameters of ~1.25 mm/s and ~2.5 mm/s, respectively, which are characteristic of high-spin Fe(II) species with oxygen and nitrogen ligation (**Figure 3**).[53] The pronounced shoulders reveal the presence of at least one additional high-spin Fe^{II} species in the sample. The 4.2-K/zero-field spectra of samples freeze-quenched at short reaction times (0.05 – 3 s, the timescale of development and decay of the transient ΔA_{320} feature in the SF-Abs experiments) after this reactant solution was mixed at 5 °C with an equal volume of O_2-saturated buffer exhibit two new features at ~0.7 mm/s and ~1.0 mm/s (red and blue arrows in **Figure 3**). These lines are at positions typically observed for the high-energy line of quadrupole doublets associated with high-spin ferryl complexes in mononuclear non-heme-iron enzymes,[7,23,33-36] suggesting that two distinct ferryl intermediates accumulate in the LolO oxacyclization reaction.

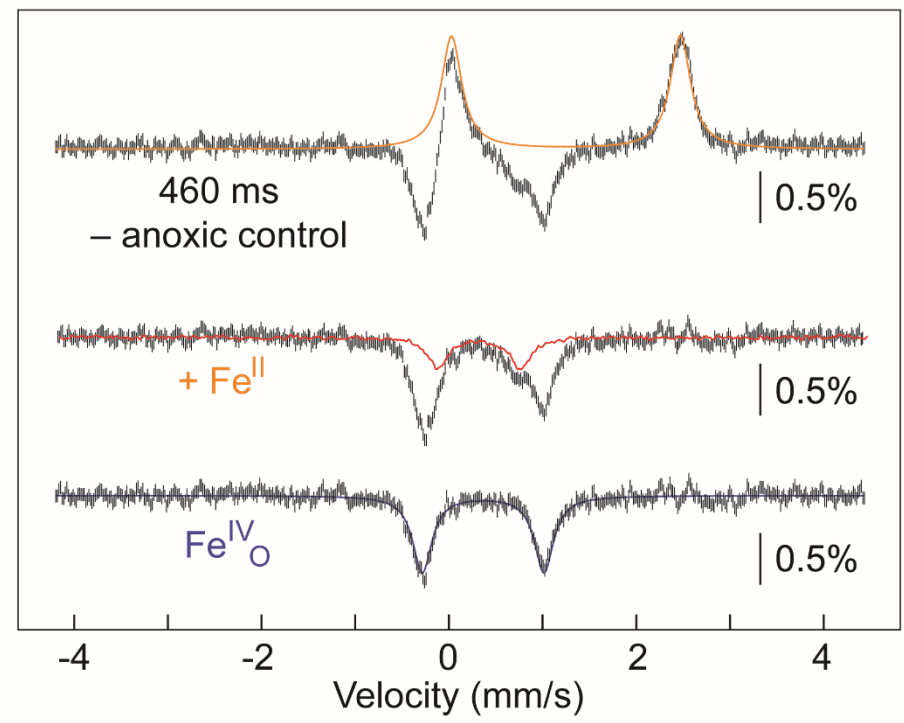

Figure 4. Generation of the spectrum of the proposed oxacyclization-initiating ferryl complex, Fe^{IV}_{O}. Experimental spectra – as well as difference spectra generated by subtracting them – are depicted as black vertical bars, with the length of each bar reflecting the error associated with that point. Simulated spectra are depicted as colored lines. Addition of the simulated spectrum of the reactant complex (orange line, top) to the difference spectrum generated by subtracting the spectrum of the reactant complex (top spectrum) from the spectrum of the 460-ms sample yields the reference spectrum of the two ferryl complexes together (middle spectrum). Removal of the features of Fe^{IV}_{H} (red line, middle; see **Figure S4**) yields the experimental reference spectrum of Fe^{IV}_{O} (bottom), which can be simulated as a quadrupole doublet with parameters $\delta = 0.36$ mm/s, $|\Delta E_Q| = 1.30$ mm/s (blue line, bottom).

To determine the parameters of the two ferryl complexes, we analyzed the spectrum of the 460 ms sample, which has the maximum total quantity of the high-valent species. We subtracted the spectrum of the reactant sample to resolve the contributions of the ferryl species (**Figure 4**, top spectrum). In this representation, the upward-pointing features are associated with decaying species (the reactant complex), and the downward-pointing features are associated with developing

species (the ferryl complexes). By adding back the quadruple doublet features of the reactant complex (**Figure 4**, top, orange line, δ = 1.24 mm/s, $|\Delta E_Q|$ = 2.44 mm/s) to the 460-ms-minus-anoxic difference spectrum yields the experimental reference spectrum of the two ferryl intermediates together (**Figure 4**, middle spectrum), in which the two lines of the major quadrupole doublet and the high-energy line of the minor quadruple doublet are clearly discernible. Importantly, the features of the minor (inner) quadrupole doublet can be modeled well with the experimental reference spectrum of the ferryl intermediate observed in the LolO-catalyzed hydroxylation reaction[7] (**Figure 4**, middle, red line; see **Figure S4** for generation of this reference spectrum); this species is denoted Fe^{IV}_H. Subtraction of the reference spectrum of Fe^{IV}_H from that of the two ferryl intermediates results in the experimental reference spectrum of the second ferryl intermediate in the oxacyclization reaction (**Figure 4**, bottom spectrum), which is denoted Fe^{IV}_O. This spectrum can be analyzed as a quadrupole doublet with unusual parameters: δ = 0.36 mm/s and $|\Delta E_Q|$= 1.30 mm/s (**Figure 4**, bottom, blue line). In particular, the isomer shift of Fe^{IV}_O is significantly greater than those of any of the other ferryl complexes characterized in Fe/2OG enzymes to date. It is, however, similar to the value of δ = 0.38 mm/s observed for the $[Fe^{IV}(O)(H_2O)_5]^{2+}$ cation,[55] lending credence to our assignment of this second species as a ferryl complex. Its anomalously high isomer shift suggests that Fe^{IV}_O has a configuration that is somehow distinct from those of Fe^{IV}_H and the ferryl complexes in the other Fe/2OG enzymes.

Next, we analogously deconvoluted the spectra of the other FQ samples using the experimentally derived reference spectra of the two ferryl intermediates. The contributions of Fe^{IV}_H and Fe^{IV}_O are shown as red and blue lines, respectively, in **Figure 3** and the quantities of each species (and their sum) determined for each reaction time are plotted in **Figure 5**.

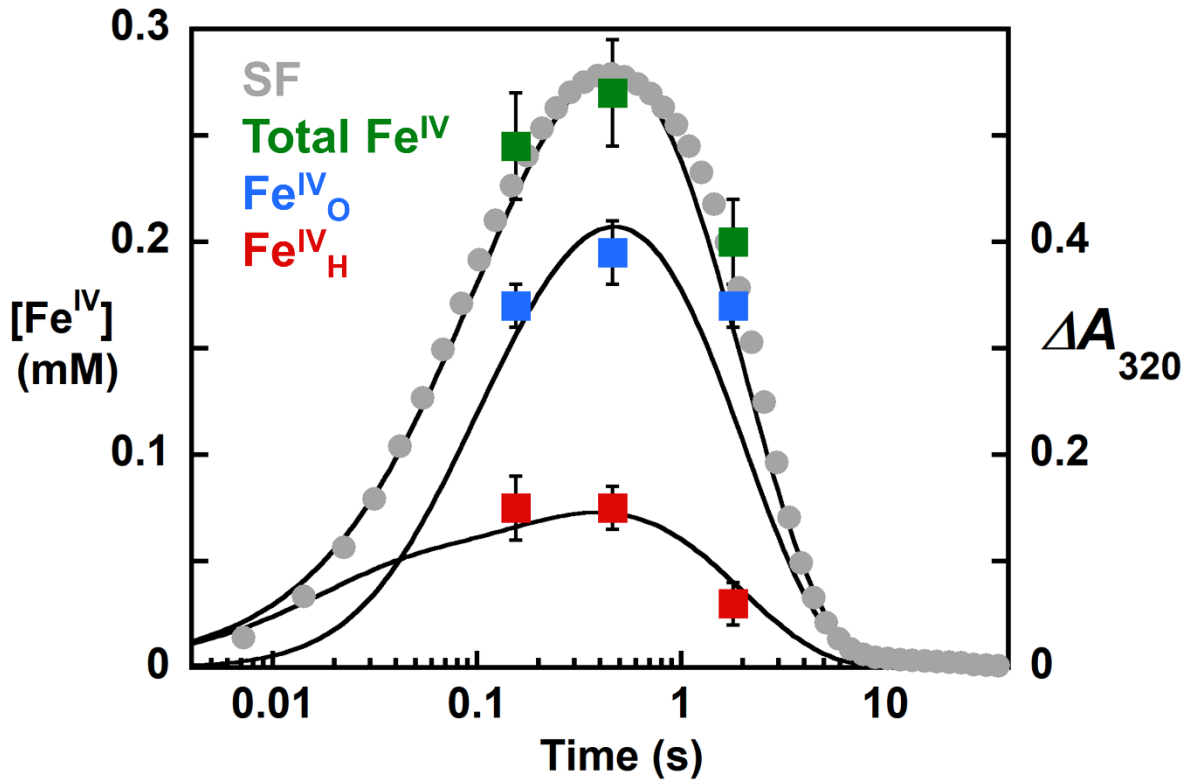

Figure 5. Comparison of the ferryl species quantified by analysis of the Mössbauer spectra of the freeze-quenched samples to the ΔA_{320}-versus-time trace obtained from an analogous SF-Abs experiment. The ΔA_{320} is shown as grey circles, total Fe^{IV} as green squares, $Fe^{IV}{}_{B}$ as blue squares, and $Fe^{IV}{}_{A}$ as red squares. The simulations (black lines) are derived from the model depicted in **Scheme S1**. In the SF-Abs experiment, a solution containing LolO (2.5 mM), Fe^{II} (2.0 mM), 2OG (7.5 mM), and 7,7-d_2-2-OH-AcAP (7 mM) was mixed with an equal volume of buffer containing ~1.2 mM O_2, giving final concentrations matching the FQ experiment (**Figure 3**). We simulated the SF-Abs traces assuming a concentration of 0.4 mM for the O_2-reactive enzyme complex (a reactive enzyme fraction of 0.4, as shown in previous analysis of LolO), and an O_2 concentration of 0.6 mM. Optimal simulation of the Mössbauer data required concentrations of 0.55 mM for O_2 and 0.36 mM for the O_2-reactive enzyme complex (a reactive fraction of 0.35), reflecting the uncertainties in these quantities.

Prior studies of the halogenases CytC3 and SyrB2 detected a pair of Fe^{IV} complexes with distinct Mössbauer spectra in each enzyme. Additional spectroscopic experiments identified them

as haloferryl species.[23,33] The ratio of the two complexes remained approximately constant in time, suggesting that they rapidly interconvert. Similarly to the situation in the halogenases, the quadrupole-doublet signatures of both ferryl complexes are evident at all reaction times in the LolO oxacyclization reaction, and the total quantity of ferryl complex (Fe^{IV}_{H} + Fe^{IV}_{O}; **Figure 5**, *green squares*) tracks well with the ΔA_{320} kinetic trace from an experiment under similar reaction conditions (*grey circles*). However, by contrast to the case of the halogenases, the ratio of the intensities of the two ferryl species in the LolO oxacylization changes significantly with time, from Fe^{IV}_{H}:Fe^{IV}_{O} ~ 1:2.3 in the 0.155-s FQ sample to Fe^{IV}_{H}:Fe^{IV}_{O} ~ 1:5.7 in the 1.8-s sample (**Figure 5**, *red and blue squares*; **Table S1**). The variable ratio of the two ferryl intermediates is best seen by comparing the intensities of the high-energy lines of Fe^{IV}_{H} and Fe^{IV}_{O} in the spectra of the 155 ms and 1.8 s samples (**Figure S6**). The kinetic data can be simulated reasonably well according to **Scheme S1A**, in which Fe^{IV}_{H} and Fe^{IV}_{O} rapidly interconvert and both have molar absorption coefficients (ε_{320}) of 2,000 $M^{-1}cm^{-1}$, the value previously determined for the single ferryl intermediate in the LolO-catalyzed hydroxylation reaction.[7] However, the agreement of the simulation with the data is somewhat improved by assumption of a kinetically significant (i.e., slower) conversion of Fe^{IV}_{H} into Fe^{IV}_{O} (**Scheme S1B**), which can accommodate the variation of the ratio of the two complexes with time. The order of their formation in **Scheme 1B** is consistent with the hypothesis that conversion of Fe^{IV}_{H} into Fe^{IV}_{O} by C2-O coordination changes the disposition of the substrate to the ferryl complex to accelerate HAT from C7 and promote coupling between C7-O and C2. This inference comports with the detection of Fe^{IV}_{H} during both reactions, but Fe^{IV}_{O} only during the oxacyclization step.

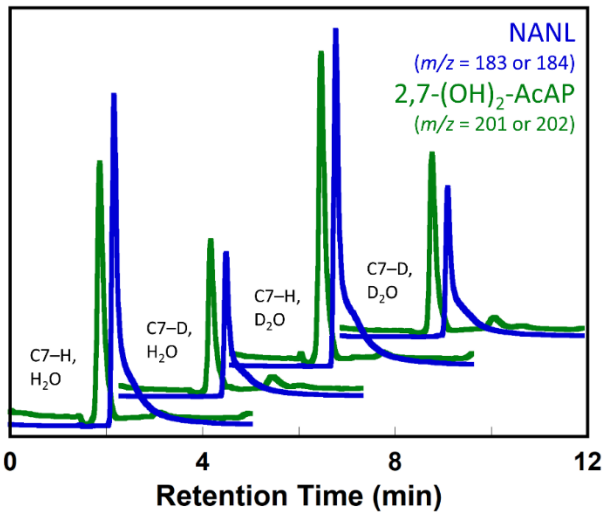

Figure 6. Relative quantities of the oxacyclization and hydroxylation products from reactions of LolO with (7-d_2-)2-OH-AcAP in H_2O and D_2O. The green traces for the dihydroxylated pyrrolizidine have all been multiplied by 18 to allow them to be compared to the blue traces for NANL. Deuterium substitution at C7 diminishes the quantity of total product as a result of uncoupling, but the cyclized product NANL is consistently favored over the dihydroxylated product 2,7-$(OH)_2$-AcAP by a factor of ~24.

Nature of the Fe(IV) species unique to the cyclization reaction. As noted, the cyclization reaction requires cleavage of both C7–H and C2-O–H bonds. In the top pathway of **Scheme 3**, the C2-O–H bond is cleaved by a proton transfer (PT) step first, followed by cleavage of the C7–H bond to generate a C7 radical, the state from which rebound and C–O coupling occur in competition. Therefore, there should be no opportunity for the presence of ^2H_2O (D_2O) solvent, which would exchange into the C2 alcohol of the substrate, to affect partitioning between the two products. In the bottom pathway of **Scheme 3**, however, the C7–H bond is cleaved first. In this pathway, the C2 hydroxyl retains its hydrogen in the C7-radical state, thus allowing for the possibility that the C–O coupling step could be delayed in D_2O solvent, resulting in an increased proportion of hydroxylation by oxygen rebound. When we performed the LolO oxacyclization reaction in D_2O,

we did not observe a significant increase in the yield of the minor hydroxylation product relative to the major cyclization product (**Figure 6**), nor did we see an effect on the kinetics of ferryl decay (**Figure S7**). As shown in a parallel study, these observations in the LolO reaction contrast with the large, normal solvent D-KIE on the product ratio and rate of ferryl decay in the H6H epoxidation reaction, for which extensive additional evidence suggests, (i) that the hydroxyl oxygen of the substrate does not coordinate to the cofactor, and (ii) that deprotonation must therefore occur after the initiating HAT step.[50]

Conclusions

Four observations reported here provide insight into the mechanism of the LolO oxacyclization reaction. First, the reaction is initiated by abstraction of H• from C7 of the 2-OH-AcAP substrate by the ferryl complex. Second, this HAT from C7 is considerably faster than the ferryl-mediated HAT from C7 of AcAP in the off-pathway hydroxylation associated with the first reaction,[52] implying a change in the relative disposition of the C7–H bond to the ferryl unit from the first to the second reaction. Third, the ferryl complex that we assign as the C7–H-cleaving intermediate in the oxacyclization reaction (because it accumulates only in that reaction) has Mössbauer parameters greater than those of any previously characterized ferryl complex in an Fe/2OG enzyme. Fourth, use of D_2O solvent impedes the bond-forming step between C2-O and C7 only to the same extent (if at all) as it impedes the competing rebound to the C7 radical, suggesting (on the basis of current understanding of the rebound step) that neither step is kinetically coupled to a proton transfer. These three observations can all be explained by coordination of the C2-O to Fe as an alkoxide. This interaction would afford a unique coordination sphere and, plausibly, distinct Mössbauer parameters. It would change the disposition of the

substrate to the high-valent complex, which could enhance HAT from C7. It would also accomplish deprotonation of the C2 hydroxyl group in advance of the initiating HAT. This explanation would imply that, after HAT from C7 to the ferryl oxygen, the C7 radical could attack the cis-coordinated alkoxyl to effect C7–O coupling by a halogenase-like radicaloid mechanism. Because sequence analysis establishes that LolO has a complete His_2-carboxylate protein ligand triad, reversible coordination of the C2 oxygen after ferryl formation but before HAT appears most likely and would explain the presence of the minor second ferryl complex with Mössbauer spectrum identical to that observed in the LolO hydroxylation reaction. In the absence of direct crystallographic evidence of C2 alkoxide coordination, which, despite our best efforts, LolO has not yet yielded, there are certainly other scenarios that could explain at least a subset of these observations. For example, a switch from in-line to off-line oxo in the second reaction could result in the different Mössbauer parameters and faster HAT from C7. However, the stark contrast of these observations to those reported in a parallel study on the H6H oxacyclization step (no rate enhancement for HAT from C7, similar and ordinary Mössbauer parameters of the first and second ferryl complexes, and a large solvent D-KIE on the cyclization/hydroxylation ratio), together with extensive structural evidence on that system that the substrate cofactor disposition does not change and the oxygen to be closed upon C7 does not coordinate, lend weight to our favored interpretation that a halogenase-like oxacyclization mechanism enabled by substrate-oxygen coordination is operant for LolO, while the H6H oxacyclization reaction proceeds by a different pathway.[50] Our ongoing efforts are directed towards obtaining more direct evidence for coordination of the 2-OH-AcAP substrate during the oxacyclization reaction using structural methods in conjunction with LolO•vanadyl complexes.[25,56]

Acknowledgements

This work was supported by the National Institutes of Health (GM113106 to J.M.B., Jr. and C.K., GM118812 to J.M.B., Jr., and GM127079 to C.K.). C.-Y.L. was supported by a grant from The Jane Coffin Childs Memorial Fund for Medical Research.

References

1. Hausinger, R. P., Fe(II)/α-ketoglutarate-dependent hydroxylases and related enzymes. *Crit. Rev. Biochem. Mol. Biol.* **2004,** *39*, 21-68.

2. Bollinger, J. M., Jr.; Chang, W.-c.; Matthews, M. L.; Martinie, R. J.; Boal, A. K.; Krebs, C., Mechanisms of 2-Oxoglutarate-Dependent Oxygenases: The Hydroxylation Paradigm and Beyond. In *2-Oxoglutarate-Dependent Oxygenases*, Hausinger, R. P.; Schofield, C. J., Eds. Royal Society of Chemistry: 2015; pp 95-122.

3. Vaillancourt, F. H.; Yin, J.; Walsh, C. T., SyrB2 in syringomycin E biosynthesis is a nonheme FeII α-ketoglutarate- and O_2-dependent halogenase. *Proc. Natl. Acad. Sci. U.S.A.* **2005,** *102*, 10111-10116.

4. Chang, W.-c.; Guo, Y.; Wang, C.; Butch, S. E.; Rosenzweig, A. C.; Boal, A. K.; Krebs, C.; Bollinger, J. M., Jr., Mechanism of the C5 stereoinversion reaction in the biosynthesis of carbapenem antibiotics. *Science* **2014,** *343*, 1140-1144.

5. Dunham, N. P.; Chang, W.-c.; Mitchell, A. J.; Martinie, R. J.; Zhang, B.; Bergman, J. A.; Rajakovich, L. J.; Wang, B.; Silakov, A.; Krebs, C.; Boal, A. K.; Bollinger, J. M., Jr., Two distinct mechanisms for C–C desaturation by iron(II)- and 2-(oxo)glutarate-dependent oxygenases: importance of α-heteroatom assistance. *J. Am. Chem. Soc.* **2018,** *140*, 7116-7126.

6. Busby, R. W.; Townsend, C. A., A single monomeric iron center in clavaminate synthase catalyzes three nonsuccessive oxidative transformations. *Bioorg. Med. Chem. Lett.* **1996,** *4*, 1059-1064.

7. Pan, J.; Bhardwaj, M.; Zhang, B.; Chang, W.-c.; Schardl, C. L.; Krebs, C.; Grossman, R. B.; Bollinger, J. M., Jr., Installation of the ether bridge of lolines by the iron- and 2-oxoglutarate-dependent oxygenase, LolO: regio- and stereochemistry of sequential hydroxylation and oxacyclization reactions. *Biochemistry* **2018,** *57*, 2074-2083.

8. Lee, H.-J.; Lloyd, M. D.; Harlos, K.; Clifton, I. J.; Baldwin, J. E.; Schofield, C. J., Kinetic and crystallographic studies on deacetoxycephalosporin C synthase (DAOCS). *J. Mol. Biol.* **2001,** *308*, 937-948.

9. Copeland, R. A.; Zhou, S.; Schaperdoth, I.; Shoda, T. K. C.; Bollinger, J. M., Jr.; Krebs, C., Hybrid radical-polar pathway for excision of ethylene from 2-oxoglutarate by an iron oxygenase. *Science* **2021,** *373*, 1489-1493.

10. Hashimoto, T.; Yamada, Y., Purification and characterization of hyoscyamine 6*β*-hydroxylase from root cultures of *Hyoscyamus niger*. *Eur. J. Biochem.* **1987,** *164*, 277-285.

11. Song, X.; Lu, J.; Lai, W., Mechanistic insights into dioxygen activation, oxygen atom exchange and substrate epoxidation by AsqJ dioxygenase from quantum mechanical/molecular mechanical calculations. *Phys. Chem. Chem. Phys.* **2017,** *19*, 20188-20197.

12. Dunham, N. P.; Del Río Pantoja, J. M.; Zhang, B.; Rajakovich, L. J.; Allen, B. D.; Krebs, C.; Boal, A. K.; Bollinger, J. M., Jr., Hydrogen donation but not abstraction by a tyrosine (Y68) during endoperoxide installation by verruculogen synthase (FtmOx1). *J. Am. Chem. Soc.* **2019**, 9964-9979.

13. Aik, W.; McDonough, M. A.; Thalhammer, A.; Chowdhury, R.; Schofield, C. J., Role of the jelly-roll fold in substrate binding by 2-oxoglutarate oxygenases. *Curr. Opin. Struct. Biol.* **2012,** *22*, 691-700.

14. Koehntop, K. D.; Emerson, J. P.; Que, L., Jr., The 2-His-1-carboxylate facial triad: A versatile platform for dioxygen activation by mononuclear non-heme iron(II) enzymes. *J. Biol. Inorg. Chem.* **2005,** *10*, 87-93.

15. Pavel, E. G.; Zhou, J.; Busby, R. W.; Gunsior, M.; Townsend, C. A.; Solomon, E. I., Circular dichroism and magnetic circular dichroism spectroscopic studies of the non-heme ferrous active site in clavaminate synthase and its interaction with α-ketoglutarate cosubstrate. *J. Am. Chem. Soc.* **1998,** *120*, 743-753.

16. Matthews, M. L.; Chang, W.-c.; Layne, A. P.; Miles, L. A.; Krebs, C.; Bollinger, J. M., Jr., Direct nitration and azidation of aliphatic carbons by an iron-dependent halogenase. *Nat. Chem. Bio.* **2014,** *10*, 209-215.

17. Neugebauer, M. E.; Sumida, K. H.; Pelton, J. G.; McMurry, J. L.; Marchand, J. A.; Chang, M. C. Y., A family of radical halogenases for the engineering of amino-acid-based products. *Nat. Chem. Bio.* **2019,** *15*, 1009-1016.

18. Slater, J. W.; Lin, C.-Y.; Neugebauer, M. E.; McBride, M. J.; Sil, D.; Nair, M. A.; Katch, B. J.; Boal, A. K.; Chang, M. C. Y.; Silakov, A.; Krebs, C.; Bollinger, J. M., Jr., Synergistic Binding of the Halide and Cationic Prime Substrate of l-Lysine 4-Chlorinase, BesD, in Both Ferrous and Ferryl States. *Biochemistry* **2023,** *62*, 2480-2491.

19. Blasiak, L. C.; Vaillancourt, F. H.; Walsh, C. T.; Drennan, C. L., Crystal structure of the non-haem iron halogenase SyrB2 in syringomycin biosynthesis. *Nature* **2006,** *440*, 368-371.

20. Zhou, J.; Gunsior, M.; Bachmann, B. O.; Townsend, C. A.; Solomon, E. I., Substrate binding to the α-ketoglutarate-dependent non-heme iron enzyme clavaminate synthase 2: coupling mechanism of oxidative decarboxylation and hydroxylation. *J. Am. Chem. Soc.* **1998,** *120*, 13539-13540.

21. Price, J. C.; Barr, E. W.; Hoffart, L. M.; Krebs, C.; Bollinger, J. M., Jr., Kinetic dissection of the catalytic mechanism of taurine:α-ketoglutarate dioxygenase (TauD) from *Escherichia coli*. *Biochemistry* **2005,** *44*, 8138-8147.

22. Neidig, M. L.; Brown, C. D.; Light, K. M.; Fujimori, D. G.; Nolan, E. M.; Price, J. C.; Barr, E. W.; Bollinger, J. M., Jr.; Krebs, C.; Walsh, C. T.; Solomon, E. I., CD and MCD of CytC3 and taurine dioxygenase: Role of the facial triad in a-KG-dependent oxygenases. *J. Am. Chem. Soc.* **2007,** *129*, 14224-14231.

23. Matthews, M. L.; Krest, C. M.; Barr, E. W.; Vaillancourt, F. H.; Walsh, C. T.; Green, M. T.; Krebs, C.; Bollinger, J. M., Jr., Substrate-triggered formation and remarkable stability of the C–H bond-cleaving chloroferryl intermediate in the aliphatic halogenase, SyrB2. *Biochemistry* **2009,** *48*, 4331-4343.

24. Li, J.; Liao, H.-J.; Tang, Y.; Huang, J.-L.; Cha, L.; Lin, T.-S.; Lee, J. L.; Kurnikov, I. V.; Kurnikova, M. G.; Chang, W.-c.; Chan, N.-L.; Guo, Y., Epoxidation Catalyzed by the Nonheme Iron(II)- and 2-Oxoglutarate-Dependent Oxygenase, AsqJ: Mechanistic Elucidation of Oxygen Atom Transfer by a Ferryl Intermediate. *J. Am. Chem. Soc.* **2020,** *142*, 6268-6284.

25. Mitchell, A. J.; Dunham, N. P.; Martinie, R. J.; Bergman, J. A.; Pollock, C. J.; Hu, K.; Allen, B. D.; Chang, W.-c.; Silakov, A.; Bollinger, J. M., Jr.; Krebs, C.; Boal, A. K., Visualizing the reaction cycle in an Iron(II)- and 2-(oxo)-glutarate-dependent hydroxylase. *J. Am. Chem. Soc.* **2017,** *139*, 13830-13836.

26. Bollinger, J. M., Jr.; Price, J. C.; Hoffart, L. M.; Barr, E. W.; Krebs, C., Mechanism of Taurine: α-Ketoglutarate Dioxygenase (TauD) from *Escherichia coli*. *EurJIC.* **2005,** *2005*, 4245-4254.

27. Mitchell, A. J.; Zhu, Q.; Maggiolo, A. O.; Ananth, N. R.; Hillwig, M. L.; Liu, X. Y.; Boal, A. K., Structural basis for halogenation by iron- and 2-oxo-glutarate-dependent enzyme WelO5. *Nat. Chem. Bio.* **2016,** *12*, 636-640.

28. Chaturvedi, S. S.; Ramanan, R.; Lehnert, N.; Schofield, C. J.; Karabencheva-Christova, T. G.; Christov, C. Z., Catalysis by the Non-Heme Iron(II) Histone Demethylase PHF8 Involves Iron Center Rearrangement and Conformational Modulation of Substrate Orientation. *ACS Catal.* **2020,** *10*, 1195-1209.

29. Borowski, T.; de Marothy, S.; Broclawik, E.; Schofield, C. J.; Siegbahn, P. E. M., Mechanism for cyclization reaction by clavaminic acid synthase. Insights from modeling studies. *Biochemistry* **2007,** *46*, 3682-3691.

30. Tamanaha, E.; Zhang, B.; Guo, Y. S.; Chang, W.-c.; Barr, E. W.; Xing, G.; St Clair, J.; Ye, S. F.; Neese, F.; Bollinger, J. M., Jr.; Krebs, C., Spectroscopic evidence for the two C-H-cleaving intermediates of *Aspergillus nidulans* Isopenicillin *N* synthase. *J. Am. Chem. Soc.* **2016,** *138*, 8862-8874.

31. Mbughuni, M. M.; Chakrabarti, M.; Hayden, J. A.; Bominaar, E. L.; Hendrich, M. P.; Münck, E.; Lipscomb, J. D., Trapping and spectroscopic characterization of an Fe(III)-superoxo intermediate from a nonheme mononuclear iron-containing enzyme. *Proc. Natl. Acad. Sci., U.S.A.* **2010,** *107*, 16788-16793.

32. Yadav, S.; Yadav, V.; Siegler, M. A.; Moënne-Loccoz, P.; Jameson, G. N. L.; Goldberg, D. P., A Nonheme Iron(III) Superoxide Complex Leads to Sulfur Oxygenation. *Journal of the American Chemical Society* **2024**.

33. Galonić, D. P.; Barr, E. W.; Walsh, C. T.; Bollinger, J. M., Jr.; Krebs, C., Two interconverting Fe(IV) intermediates in aliphatic chlorination by the halogenase CytC3. *Nat. Chem. Bio.* **2007,** *3*, 113-116.

34. Hoffart, L. M.; Barr, E. W.; Guyer, R. B.; Bollinger, J. M., Jr.; Krebs, C., Direct spectroscopic detection of a C–H-cleaving high-spin Fe(IV) complex in a prolyl-4-hydroxylase. *Proc. Natl. Acad. Sci. U.S.A.* **2006,** *103*, 14738-14743.

35. Copeland, R. A.; Davis, K. M.; Shoda, T. K. C.; Blaesi, E. J.; Boal, A. K.; Krebs, C.; Bollinger, J. M., Jr., An Iron(IV)–Oxo Intermediate Initiating L-Arginine Oxidation but Not Ethylene Production by the 2-Oxoglutarate-Dependent Oxygenase, Ethylene-Forming Enzyme. *J. Am. Chem. Soc.* **2021,** *143*, 2293-2303.

36. Price, J. C.; Barr, E. W.; Tirupati, B.; Bollinger, J. M., Jr.; Krebs, C., The first direct characterization of a high-valent iron intermediate in the reaction of an a-ketoglutarate-dependent dioxygenase: A high-spin Fe(IV) complex in taurine/a-ketoglutarate dioxygenase (TauD) from *Escherichia coli*. *Biochemistry* **2003,** *42*, 7497-7508.

37. Sinnecker, S.; Svensen, N.; Barr, E. W.; Ye, S.; Bollinger, J. M., Jr.; Neese, F.; Krebs, C., Spectroscopic and computational evaluation of the structure of the high-spin Fe(IV)-oxo intermediates in taurine:α-ketoglutarate dioxygenase from *Escherichia coli* and its His99Ala ligand variant. *J. Am. Chem. Soc.* **2007,** *129*, 6168-6179.

38. Groves, J. T., Key elements of the chemistry of cytochrome P-450: the oxygen rebound mechanism. *J. Chem. Educ.* **1985,** *62*, 928-931.

39. Brunson, J. K.; McKinnie, S. M. K.; Chekan, J. R.; McCrow, J. P.; Miles, Z. D.; Bertrand, E. M.; Bielinski, V. A.; Luhavaya, H.; Oborník, M.; Smith, G. J.; Hutchins, D. A.; Allen, A. E.; Moore, B. S., Biosynthesis of the neurotoxin domoic acid in a bloom-forming diatom. *Science* **2018,** *361*, 1356-1358.

40. Jakubczyk, D.; Caputi, L.; Stevenson, C. E. M.; Lawson, D. M.; O'Connor, S. E., Structural characterization of EasH (*Aspergillus japonicus*) – an oxidase involved in cycloclavine biosynthesis. *Chem. Commun.* **2016,** *52*, 14306-14309.

41. Matthews, M. L.; Neumann, C. S.; Miles, L. A.; Grove, T. L.; Booker, S. J.; Krebs, C.; Walsh, C. T.; Bollinger, J. M., Jr., Substrate positioning controls the partition between halogenation and hydroxylation in the aliphatic halogenase, SyrB2. *Proc. Natl. Acad. Sci. U.S.A.* **2009,** *106*, 17723-17728.

42. Martinie, R. J.; Livada, J.; Chang, W.-c.; Green, M. T.; Krebs, C.; Bollinger, J. M., Jr.; Silakov, A., Experimental correlation of substrate position with reaction outcome in the aliphatic halogenase, SyrB2. *J. Am. Chem. Soc.* **2015,** *137*, 6912-6919.

43. Srnec, M.; Solomon, E. I., Frontier molecular orbital contributions to chlorination versus hydroxylation selectivity in the non-heme iron halogenase SyrB2. *J. Am. Chem. Soc.* **2017,** *139*, 2396-2407.

44. Dunham, N. P.; Arnold, F. H., Nature's Machinery, Repurposed: Expanding the Repertoire of Iron-Dependent Oxygenases. *ACS Catal.* **2020,** *10*, 12239-12255.

45. Cheung-Lee, W. L.; Kolev, J. N.; McIntosh, J. A.; Gil, A. A.; Pan, W.; Xiao, L.; Velásquez, J. E.; Gangam, R.; Winston, M. S.; Li, S.; Abe, K.; Alwedi, E.; Dance, Z. E. X.; Fan, H.; Hiraga, K.; Kim, J.; Kosjek, B.; Le, D. N.; Salehi Marzijarani, N.; Mattern, K.; McMullen, J. P.; Narsimhan, K.; Vikram, A.; Wang, W.; Yan, J.-X.; Yang, R.-S.; Zhang, V.; Zhong, W.; DiRocco,

D. A.; Morris, W. J.; Murphy, G. S.; Maloney, K. M., Engineering Hydroxylase Activity, Selectivity, and Stability for a Scalable Concise Synthesis of a Key Intermediate to Belzutifan. *Angew. Chem. Int. Ed.*

46. Hashimoto, T.; Yamada, Y., Hyoscyamine 6-beta-hydroxylase, a 2-oxoglutarate-dependent dioxygenase, in alkaloid-producing root cultures. *Plant Physiol.* **1986,** *81*, 619-625.

47. Hashimoto, T.; Matsuda, J.; Yamada, Y., 2-Step epoxidation of hyoscyamine to scopolamine is catalyzed by bifunctional hyscyamine 6-beta-hydroxylase. *FEBS Lett.* **1993,** *329*, 35-39.

48. Orville, A. M.; Chen, V. J.; Kriauciunas, A.; Harpel, M. R.; Fox, B. G.; Münck, E.; Lipscomb, J. D., Thiolate ligation of the active site iron(II) of isopenicillin N synthase derives from substrate rather than endogenous cysteine: spectroscopic studies of site-specific Cys .fwdarw. Ser mutated enzymes. *Biochemistry* **1992,** *31*, 4602-12.

49. Panth, N.; Wenger, E. S.; Krebs, C.; Bollinger, J. M., Jr.; Grossman, R. B., Synthesis of 6,6- and 7,7-Difluoro-1-acetamidopyrrolizidines and Their Oxidation Catalyzed by the Nonheme Fe Oxygenase LolO. *Chembiochem* **2022,** *23*.

50. Wenger, E. S.; Martinie, R. J.; Ushimaru, R.; Pollock, C. J.; Sil, D.; Li, A.; Nhi, H.; Palowitch, G. M.; Graham, B. P.; Schaperdoth, I.; Burke, E. J.; Maggiolo, A. O.; Allen, B. D.; Krebs, C.; Silakov, A.; Boal, A. K.; Bollinger, J. M., Jr., Optimized Substrate Positioning Enables Switches in C–H Cleavage Site and Reaction Outcome in the Hydroxylation-Epoxidation Sequence Catalyzed by Hyoscyamine 6β-Hydroxylase. *ChemRxiv.* **2024,** doi:10.26434/chemrxiv-2024-jkhk9.

51. Neugebauer, M. E.; Kissman, E. N.; Marchand, J. A.; Pelton, J. G.; Sambold, N. A.; Millar, D. C.; Chang, M. C. Y., Reaction pathway engineering converts a radical hydroxylase into a halogenase. *Nat. Chem. Bio.* **2022,** *18*, 171-179.

52. Pan, J.; Wenger, E. S.; Matthews, M. L.; Pollock, C. J.; Bhardwaj, M.; Kim, A. J.; Allen, B. D.; Grossman, R. B.; Krebs, C.; Bollinger, J. M., Jr., Evidence for Modulation of Oxygen Rebound Rate in Control of Outcome by Iron(II)- and 2-Oxoglutarate-Dependent Oxygenases. *J. Am. Chem. Soc.* **2019,** *141*, 15153-15165.

53. Münck, E., Aspects of ^{57}Fe Mössbauer spectroscopy. In *Physical Methods in Bioinorganic Chemistry*, Que, L., Jr., Ed. University Science Books: Sausalito, CA, 2000; pp 287-319.

54. Bollinger, J. M., Jr.; Krebs, C., Stalking intermediates in oxygen activation by iron enzymes: Motivation and method. *J. Inorg. Biochem.* **2006,** *100*, 586-605.

55. Pestovsky, O.; Stoian, S.; Bominaar, E. L.; Shan, X.; Münck, E.; Que Jr., L.; Bakac, A., Aqueous FeIV=O: Spectroscopic Identification and Oxo-Group Exchange. *Angew. Chem. Int. Ed.* **2005,** *44*, 6871-6874.

56. Martinie, R. J.; Pollock, C. J.; Matthews, M. L.; Bollinger, J. M., Jr.; Krebs, C.; Silakov, A., Vanadyl as a Stable Structural Mimic of Reactive Ferryl Intermediates in Mononuclear Nonheme-Iron Enzymes. *Inorganic Chemistry* **2017,** *56*, 13382-13389.